Modeling of a Loop Thermosyphon Supplying Solar Energy to a Desalination Boiler

Josh Charles[1, a)], Nathan Van Velson[1, b)], Jianjian Wang[1, c)], Sean Hoenig[1, d)]

[1]*Advanced Cooling Technologies, 1046 New Holland Ave., Lancaster, PA 17601, USA, 1-717-295-6061*

[a)]*josh.charles@1-act.com*
[b)]*nathan.vanvelson@1-act.com*
[c)]*jianjian.wang@1-act.com*
[d)]*sean.hoenig@1-act.com*

Abstract. A new concentrated solar desalination system based on a two-phase working fluid with volumetric solar absorption is under development. This system promises to improve overall solar to thermal efficiency and reduce parasitic power by taking advantage of the passive flow circulation of a loop thermosyphon. To predict system performance, a two-phase loop thermosyphon model was developed around well-validated, two-phase frictional pressure drop correlations. The model was used to analyze pressure drops and resulting fluid saturation temperatures throughout the loop. Good agreement was found between predicted fluid mass flow rate and that measured in a lab-scale loop thermosyphon prototype. The model continues to be developed and will be validated against a larger-scale prototype system.

INTRODUCTION

Concentrated solar power (CSP) is an attractive option for providing process heat for saltwater desalination. This heat can be used for brine distillation or brine heating upstream of a reverse osmosis membrane. Most CSP systems utilize parabolic trough solar concentrators coupled with steel evacuated tube receivers. This CSP configuration experiences optical losses across the trough and transmittance and heat transfer losses within the receiver. At the system level, there are heat transfer losses from the field tubing to the environment, and a significant parasitic pumping power requirement. To minimize receiver and pumping power efficiency losses, Advanced Cooling Technologies (ACT) has designed a solar thermal desalination system with a new solar receiver and heat transfer fluid (HTF), where the pump is eliminated through use of a passively driven, two-phase loop thermosyphon (Fig. 1).

ACT's desalination solar collector improves on the state of the art (SOA) in three key areas. First, the vacuum insulated steel receiver is replaced by a vacuum insulated glass receiver, which allows the solar radiation to directly impinge on and be absorbed by the working fluid. This change eliminates conductive and convective losses across the receiver tube wall. Selection of an appropriate working fluid is critical as the working fluid must achieve close to 100% volumetric solar spectral absorptance and maintain performance over prolonged thermal and UV exposure. Through life-testing, ACT is evaluating several promising working fluids with potential for good long-term performance. Modeling suggests that the volumetric solar receiver will improve the solar to thermal conversion efficiency by around 2% (absolute) over an SOA receiver.

The second key improvement is the use of a two-phase working fluid between the receiver outlet and brine heater. Ideally, the working fluid leaves the receiver with between a 50 and 70% void fraction, allowing it to efficiently absorb incident radiation along the entire length of the receiver. By storing thermal energy in the latent heat of the working fluid, the same quantity of thermal energy can be transferred at a reduced working fluid temperature and flow rate. This lower operating temperature reduces thermal losses to the ambient between the receiver and brine heater.

Condensing flow within the brine heater also allows for a reduction in heat exchanger area as the condensing heat transfer rate is improved relative to that of a single-phase working fluid.

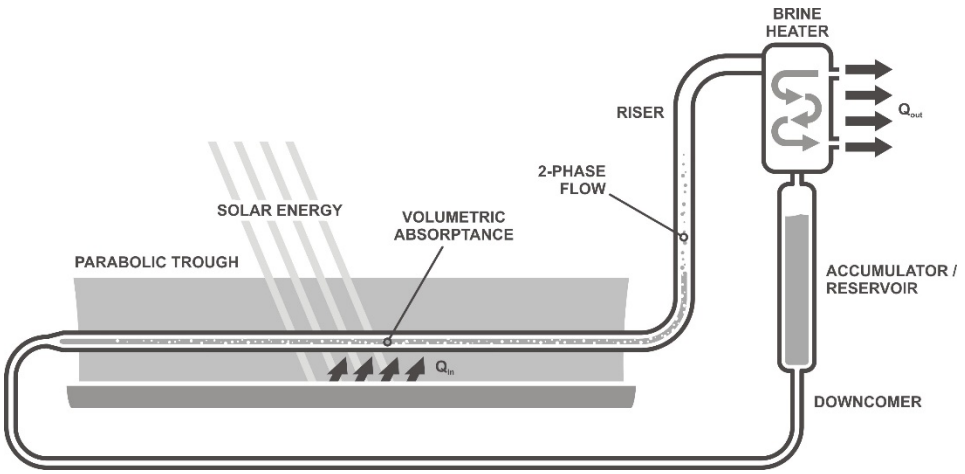

FIGURE 1: Solar Thermal Loop Thermosyphon for Saltwater Desalination.

The final improvement (and focus of this paper) is due to the potential for the two-phase system to operate as a loop thermosyphon (LTS). A loop thermosyphon utilizes the density difference between a two-phase riser and condensate downcomer to provide fluid circulation without a pump. Preliminary thermo-economic modeling suggests that eliminating the pump reduces lifetime levelized capital, operating, and maintenance costs by about 19%.

LOOP THERMOSYPHON THEORY

A loop thermosyphon is a specialized configuration of a single-tube thermosyphon. In a thermosyphon, a working fluid absorbs heat and boils in an evaporative region. Evaporated vapor buoyantly rises along the tube to the condenser, where it condenses, releasing thermal energy. Condensed liquid returns to the evaporator via gravity, falling along the walls of the thermosyphon counter-current to the vapor flow. The operation of a traditional thermosyphon is illustrated in Fig. 2 (a). The flooding limit constrains the maximum power of a thermosyphon, and is imposed by shear forces between a high-velocity, upward vapor flow and downward liquid return flow.

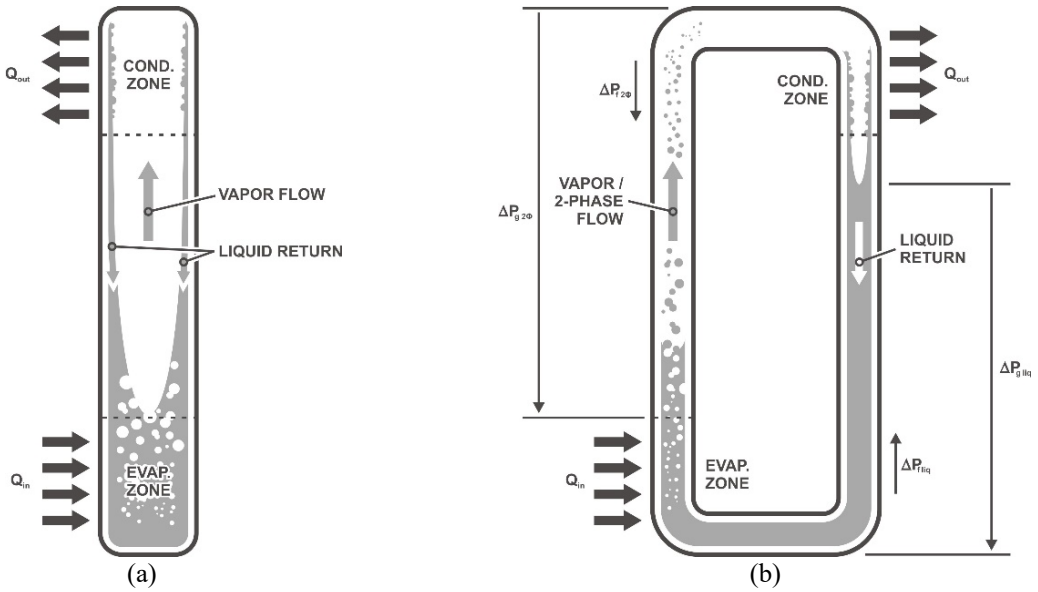

FIGURE 2. (a) Traditional Thermosyphon Operation vs. (b) Loop Thermosyphon Operation.

The flooding limit can be bypassed by using a loop thermosyphon. LTS operation is illustrated in Fig. 2 (b). As in a traditional thermosyphon, heat applied in the evaporator zone boils the working fluid, which rises to the condenser. Unlike a traditional thermosyphon, when the working fluid is condensed, the liquid returns to the evaporator in a line separate from the rising vapor phase. With separate vapor and liquid lines, shear between the phases is eliminated, removing the flooding limit constraint. One feature of an LTS is that it is possible for a two-phase working fluid to flow against gravity from evaporator to condenser. In other words, liquid can be carried along with the vapor leaving the evaporator. The motive force required to lift this liquid is provided by the gravitational head of the liquid condensate beneath the condenser ($\Delta P_{g\,liq}$). Resisting this positive head is the gravitational head of the two-phase flow ($\Delta P_{g\,2\phi}$) and frictional pressure drops in the liquid ($\Delta P_{f\,liq}$) and two-phase lines ($\Delta P_{f\,2\phi}$). In addition, the sum of acceleration ($\Sigma\Delta P_a$) and minor pressure losses ($\Sigma\Delta P_m$) also resist the fluid flow and must be accounted for. During steady-state loop thermosyphon operation, these six pressure components must be in equilibrium:

$$\Delta P_{g\,liq} + \Delta P_{g\,2\phi} + \Delta P_{f\,liq} + \Delta P_{f\,2\phi} + \Sigma\Delta P_a + \Sigma\Delta P_m = 0 \tag{1}$$

Equation (1) forms the basis for modeling of LTS performance and can be applied a wide range of LTS geometries, working fluids, and input powers. By predicting gravitational, frictional and acceleration pressure drops around an LTS, the model can predict changes in the saturation temperature, which directly influence the working fluid thermal resistance between the evaporator and condenser.

LOOP THERMOSYPHON MODEL DESIGN

Beginning from the pressure balance principle of Eqn. (1), a numeric mass and energy balance model of the solar-driven LTS was created. Within the code, the LTS is initially divided into discrete sections for sequential analysis. The following four types of sections were defined within the model: evaporator sections, condenser sections, tube sections, and elbows. An example of this loop thermosyphon discretization is illustrated in Fig. 3 alongside critical dimensions and fluid operating parameters defined and calculated by the model.

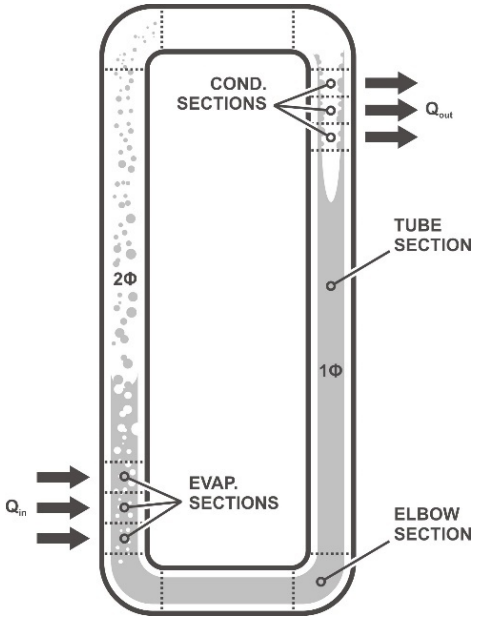

DIMENSIONS
- ID: Inner Diameter
- OD: Outer Diameter
- L: Length
- A: Cross-sectional Area
- θ: Tube Inclination (relative to positive x-axis)
- r: Elbow Radius

BASE FLUID PARAMETERS
- h: Enthalpy
- P: Pressure

DERIVATIVE FLUID PARAMETERS
- T: Temperature
- ρ: Density
- μ: Viscosity
- σ: Surface Tension

CALCULATED FLUID PARAMETERS
- ΔP_f: Frictional Pressure Drop
- ΔP_g: Gravitational Head
- ΔP_a: Acceleration Pressure Drop
- ΔP_m: Minor Pressure Losses
- α: Void Fraction
- h_c Convective Heat Transfer Coefficient

FIGURE 3. Illustration of LTS Model Discretization and Important Calculation Dimensions and Parameters.

Model execution begins by specifying a saturation temperature, operating temperature (if superheated or subcooled), and fluid quality, which define the enthalpy and pressure at the inlet or outlet of the starting section. Beginning from this point of the loop, a heat and mass balance is serially performed alongside a pressure drop analysis for each section of the loop. The fluid flow is fully defined by only two "base" parameters; enthalpy and pressure. The

model iterates on these two parameters with temperature, density, viscosity, and surface tension derived from the pressure and enthalpy values in each section.

Frictional Pressure Drop Calculations

As suggested by Eqn. (1), accurate calculation of the loop pressure drops is essential in predicting the performance of the LTS. In sections with single-phase liquid or vapor (i.e. in the downcomer), frictional pressure drop is calculated using the standard Darcy frictional factor equation for tubular flow. However, in the evaporator, two-phase riser, and condenser, empirically derived, two-phase pressure drop correlations are most applicable.

Lockhart and Martinelli (L-M) [1] proposed that the two-phase frictional pressure drop per unit length $(dP_f/dz)^{2\phi}$ be estimated by multiplying the single-phase frictional pressure drop for the liquid phase $(dP_f/dz)_{liq}$ by a two-phase frictional pressure drop multiplier ($\phi_{liq}^{2\phi}$):

$$\left(\frac{dP_f}{dz}\right)^{2\phi} = \phi_{liq}^{2\phi}\left(\frac{dP_f}{dz}\right)_{liq} \tag{2}$$

The two-phase frictional pressure drop multiplier is a function of the Lockhart and Martinelli parameter (*XLM*) and a *C* value (Table 1)

$$\phi_{liq}^{2\phi} = 1 + \frac{C}{XLM} + \frac{1}{XLM^2} \tag{3}$$

TABLE 1. C Values for the L-M Correlation [2]

		Vapor	
		Lam.	Turb.
Liquid	Lam.	5	10
	Turb.	12	20

The *XLM* parameter is defined as the ratio of the pressure drops if the liquid and vapor flow rates are individually filling the entire flow cross section:

$$XLM = \sqrt{\frac{\left(\frac{dP_f}{dz}\right)_{liq}}{\left(\frac{dP_f}{dz}\right)_{vap}}} \tag{4}$$

The single-phase pressure drops are calculated using the single-phase Darcy pressure drop equation for liquid or vapor flow:

$$\left(\frac{dP_f}{dL}\right)_{liq} = \frac{2f_{liq}G^2(1-x)^2}{d_h\rho_{liq}} \qquad \left(\frac{dP_f}{dL}\right)_{vap} = \frac{2f_{vap}G^2x^2}{d_h\rho_{vap}} \tag{5} \& (6)$$

Where, G is the mass velocity ($\dot{m}/A$) of the entire flow, x is the quality, and d_h is the hydraulic diameter. A transition Reynolds number of 2,300 was assumed in calculating the laminar and turbulent friction factors:

$$f_{lam} = \frac{64}{Re_{liq/vap}} \qquad f_{turb} = \frac{0.316}{Re_{liq/vap}^{0.25}} \tag{7} \& (8)$$

Finally, Reynolds numbers for the liquid and vapor portion of the flow are calculated using the mass velocity and quality according to Equations (9) and (10):

$$Re_{liq} = \frac{\rho_{liq} G(1-x) d_h}{\mu_{liq}} \qquad Re_{vap} = \frac{\rho_{vap} G x d_h}{\mu_{vap}} \qquad (9)\ \&\ (10)$$

Equations (2) through (10) are used by the model to predict the two-phase frictional pressure drop. The *C* values presented by Chisholm in Table 1 only apply to horizontal, tubular two-phase flow. Yadav expanded on this work, by studying fully-turbulent, vertical upward and downward two-phase flows, with appropriate *C* values for both cases proposed [3]. A linear curve fit between Chisholm's horizontal *C* values (0°) and Yadav's values for ±90° was used to create an equation for the turbulent liquid-turbulent vapor (*tl-tv*) *C* value at any tube inclination (θ):

$$\text{For } \theta \text{ between 0 and 90°: } C_{tl-tv} = 0.22\bar{\theta} + 20 \qquad (11)$$

$$\text{For } \theta \text{ between 270 and 360°: } C_{tl-tv} = 0.11\bar{\theta} - 20 \qquad (12)$$

Where, θ is in degrees. In addition to the L-M correlation, the Friedel two-phase frictional pressure drop correlation was also implemented in the model. The correlation used is user-selectable in the model user interface. Complete details of the Friedel correlation are outlined by Filip et al. [4].

An accurate prediction of void fraction (α) throughout the two-phase flow is critical to accurate estimations of fluid charge. Several user-selectable methods for estimating void fraction in the two-phase region were implemented in the model. These include Lockhart and Martinelli's method based on the previously defined *XLM* parameter:

$$\alpha = \left(1 + XLM^{0.8}\right)^{-0.378} \qquad (13)$$

Heat Transfer Calculations

To estimate thermal losses from the thermosyphon and better predict heat transfer within the evaporator and condenser, heat transfer coefficients were calculated throughout the single and two-phase sections of the loop. Within the evaporator, a correlation developed by Kandlikar was used to predict the saturated flow boiling heat transfer coefficient ($h_{2\phi b}$). This boiling heat transfer coefficient is a function of the convective (*Co*) and boiling (*Bo*) numbers, the single-phase liquid heat transfer coefficient (h_{liq}), a fluid parameters (F_{fl}), the liquid only Froude number (Fr_{LO}), and five constants (C_1-C_5):

$$h_{2\phi b} = C_1 Co^{C_2} (25 Fr_{LO})^{C_5} h_{liq} + C_3 Bo^{C_4} h_{liq} F_{fl} \qquad (14)$$

The calculation of these values is beyond the scope of this paper, but complete details are presented by Kandlikar [5]. In the non-boiling, two-phase region, Chen's modified form of the Dittus-Boelter equation is used to calculate the two-phase heat transfer coefficient ($h_{2\phi}$) [6]:

$$h_{2\phi} = 0.023\,(Re_m)^{0.8} \left(Pr_{liq}\right)^{0.4} \frac{k_{liq}}{d_h} \qquad (15)$$

Where, Re_m is the homogeneous mixture Reynolds number. For loop thermosyphon sections in the condenser, the Shah correlation was chosen to approximate the condensing heat transfer coefficient. As presented by Papini et al. [7], the local, two-phase condensing heat transfer coefficient ($h_{2\phi c}$) can be computed by another Dittus-Boelter-based correlation:

$$h_{2\phi c} = h_{liq} \left[(1-x)^{0.8} + \frac{3.8 x^{0.76} (1-x)^{0.04}}{Pr_{liq}^{0.38}} \right] \qquad (16)$$

Shah's correlation, presented in Eqn. (16), is applicable to vertical, inclined, and horizontal condensers. After solving for the heat transfer coefficient around the loop thermosyphon, heat loss from each section is estimated using a sum of thermal resistance method through the tube wall and an insulation layer surrounding the tube.

LAB-SCALE SOLAR THERMAL COLLECTOR

The pressure drop and heat transfer model was used to model a lab-scale version of the loop thermosyphon for concentrated solar desalination. The geometry of this model is illustrated in Fig. 4 (a). A 0.5 m horizontal evaporator was located ~0.3 m below the midpoint of the condenser. 15.7 mm ID tubing was used throughout, with a constriction to 8 mm through the flow meter located in the liquid return line.

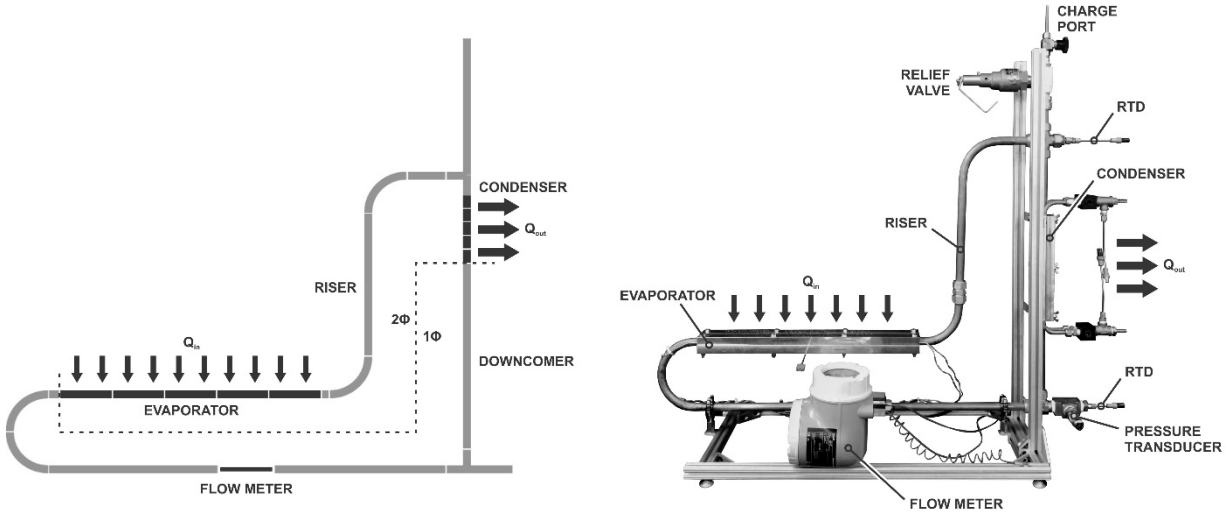

(a) (b)

FIGURE 4. (a) Model Illustration of Lab-Scale Solar LTS, (b) Constructed Lab-Scale Solar LTS.

Before constructing the lab-scale prototype [Fig. 4 (b)], the model was used to verify system performance at evaporator powers between 200 and 900 W and saturation temperatures of 100, 110, and 120°C. Predicted flow rate and evaporator exit void fraction for these conditions are presented in Fig. 5 (a).

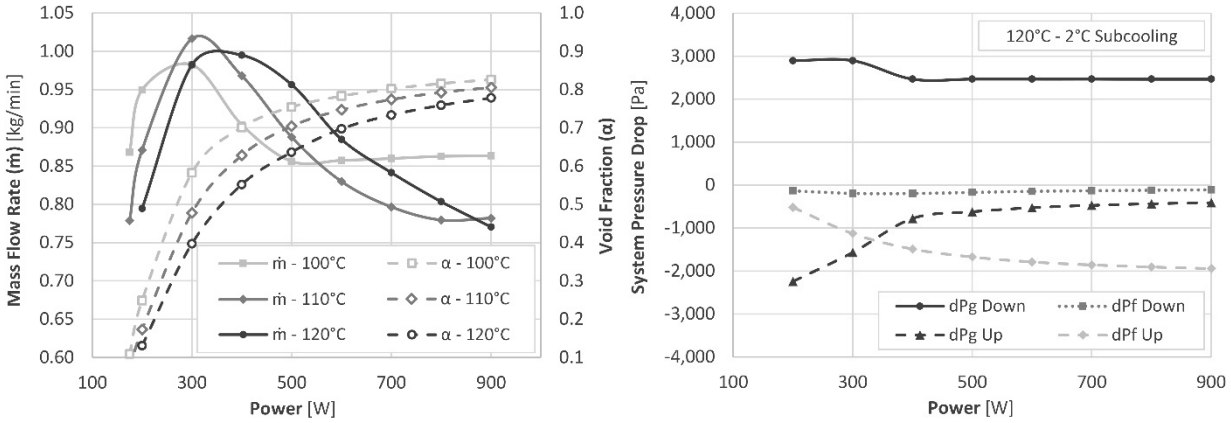

(a) (b)

FIGURE 5. (a) Mass Flow Rates and (b) Key Pressure Drops Calculated by Model for Lab-Scale System.

Figure 5 (a) shows that at each operating temperature, flow rate initially increases with power before peaking and falling at powers greater than 300-400 W. Void fraction rapidly increases at powers less than ~400 W, but the curve flattens at higher powers. To better understand the peak in mass flow rate at 300-400 W, the gravitational head and frictional pressure drops for the two-phase riser (Up) and liquid phase downcomer (Down) are presented in Fig. 5 (b) for a 120°C working fluid. At powers less than 300-400 W, Fig. 5 (b) shows that the gravitational head of the two-phase riser is the dominate pressure drop opposing the driving liquid head of the downcomer. This is due to the low

void fraction at low powers. As power increases from 200 W, the two-phase void fraction rapidly increases, driving the two-phase head down. This rapid decrease in two-phase head is responsible for the initial increase in flow rate with increasing power. However, as power and two-phase void fraction continue to rise, the two-phase frictional pressure drop begins to increase. Eventually, the decrease in two-phase head is completely offset by the increase in two-phase frictional pressure drop and this point corresponds to the peak mass flow rate seen in Fig. 5 (a).

The lab-scale system presented in Fig. 4 (b) was fabricated from copper tubing with heat supplied by four cartridge heaters fitting into aluminum blocks clamped around the evaporative section of the loop. The condenser was similarly constructed with two aluminum blocks clamped around the LTS tube and two parallel coolant tubes. Chilled water was supplied to the condenser via a chiller, with a flow meter and resistance temperature detectors (RTDs) used to quantify the thermal energy removed in the condenser. LTS temperatures were recorded via RTDs located at the entrance of the condenser and bottom of the downcomer, with pressure at the bottom of the downcomer measured via an absolute pressure transducer. An electromagnetic flow meter was located in the liquid return line to record the working fluid flow rate. The system was leak tested under vacuum before being charged with between 650 and 850 ml of deionized water. Evaporator power was varied between 500 and 1,000 W with the coolant flow rate controlled such that the LTS saturation temperature was held constant. Experimental mass flow rate (Exp.) is plotted vs. power for the three experimental fluid charges in Fig. 6.

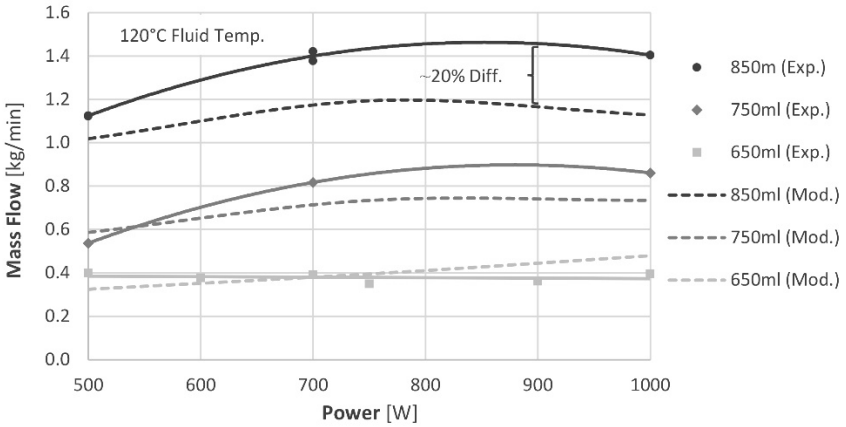

FIGURE 6. Experimental vs. Modeled Mass Flow Rate Results for Lab-Scale LTS.

As expected, mass flow rate was found to directly correlate with charge. A greater fluid charge corresponds to a greater liquid head in the downcomer, increasing the working fluid motive force and resulting flow rate. Modeled flow rate results (Mod.) for the lab-scale system are presented alongside the experimental data in Fig. 6. Experimental and modeled results were found to agree very well at charges of 650 and 750 ml. At 850 ml, a maximum difference of ~20% was found between the experimental and modeled mass flow rates. This is within the typical uncertainty range of the two-phase pressure drop correlations used in the model. Importantly, the results in Fig. 6 show that the trend of increasing flow rate with increasing charge is accurately predicted by the model.

CONCLUSIONS & NEXT STEPS

This work shows that the new two-phase LTS model can predict the performance of the solar desalination LTS under development. While a maximum mass flow rate difference of ~20% was found between the experimental and model results, this is within the prediction uncertainty of the two-phase Lockhart and Martinelli pressure drop correlation used in the model. One limitation of the current lab-scale LTS is that it only allowed for accurate mass flow rate comparison with the model due to limited temperature and pressure instrumentation. To address this issue, a larger, sub-scale LTS is under construction with complete temperature and pressure instrumentation at the inlet and outlet of the evaporator and condenser. This system will allow for comparison of flow rate, temperature, and sectional pressure drops between the experiment and model. The larger tube diameter and system size will also allow the model to be validated across a broader range of system sizes and operating parameters.

ACKNOWLEDGMENTS

This work was performed for the Solar Energy Technology Office (SETO) under contract number DE-EE000839. The technical monitor is Mark Lausten. The authors would like to acknowledge Phil Texter, Julian Lorah, and Larry Waltman for their assistance in the design, assembly and testing of the lab-scale loop thermosyphon.

REFERENCES

1. R. W. Lockhart and R. C. Martinelli, "Proposed Correlation of Data for Isothermal Two-Phase Two-Component Flow in Pipes," in *Chemical Engineering Progress, 45*(1), 1949, pp. 39-48.
2. D. Chisholm, "A Theoretical Basis for the Lockhart-Martinelli Correlation for Two-Phase Flow," in *International Journal of Heat and Mass Transfer 10,* 1967, pp. 1767-1778.
3. M.S. Yadav, "Interfacial Area Transport Across Vertical Elbows in Air-Water Two-Phase Flow," PhD thesis, Pennsylvania State University, 2013.
4. A. Filip and R. D. Bălțăreţu, "Comparison of Two-Phase Pressure Drop Models for Condensing Flows in Horizontal Tubes." in *Mathematical Modeling in Civil Engineering, 10*(4), 2014, pp. 19-27.
5. S. G. Kandlikar, "A General Correlation for Saturated Two-Phase Flow Boiling Heat Transfer Inside Horizontal and Vertical Tubes," in *Journal of Heat Transfer, 112*, 1990, pp. 219-228.
6. J.C. Chen, "A Correlation for Boiling Heat Transfer to Saturated Fluids in Convective Flow," Brookhaven National Laboratory, Upton, NY, 1962.
7. D. Papini, A. Cammi, “Modelling of Heat Transfer Phenomena for Vertical and Horizontal Configurations of In-Pool Condensers and Comparison with Experimental Findings,” in *Science and Technology of Nuclear Installation,* 2010.